Titania−Silica: A Model Binary Oxide Catalyst System

Robert J. Davis* and Zhufang Liu†

Department of Chemical Engineering, University of Virginia, Charlottesville, Virginia 22903-2442

Received May 2, 1997. Revised Manuscript Received June 30, 1997⊗

Titania−silica mixed oxides are intriguing catalysts and catalyst supports since their surface reactivities depend strongly on composition and homogeneity of mixing. In this review, the synthesis, characterization, and catalytic activity of titania−silica are described, and important structure/property relationships for these materials are emphasized.

I. Introduction

A major focus of current catalysis research is the elucidation of critical structure/function relationships for existing solid catalysts that can be subsequently utilized in the rational design of new materials. These studies necessarily combine expertise in materials synthesis, characterization, and catalytic testing. Since research of this nature is inherently interdisciplinary, future advances in catalyst design will most likely result from teams of researchers that bring a variety of skills to the area. In this paper, we illustrate the importance of all three facets of catalytic materials research (synthesis, characterization, and testing) for titania-silica mixed oxides, solids that have attracted considerable attention as advanced materials, heterogeneous catalysts, and catalyst supports. For example, silica glasses containing trace quantities of Ti are used in fibers, films, and optical mirrors since these materials exhibit very low coefficients of thermal expansion over a wide temperature range.[1,2] In addition, certain compositions of the Ti−Si mixed oxides are active for acid-catalyzed reactions such as phenol amination,[3] ethene hydration,[3] butene isomerization,[3−5] cumene dealkylation,[6] 2-propanol dehydration,[6] and 1,2-dichloroethane decomposition.[7] Other compositions of these materials are known to be effective for selective oxidation reactions using organic hydroperoxides as the oxygen source.[8] The diversity of reactions catalyzed by titania-silica mixed oxides makes this system ideal for fundamental studies into the structure/function relationships necessary for metal oxide catalysis.

Throughout the 1990s, our research group has investigated in detail the microstructural characteristics and catalytic reactivity of a wide range of amorphous titania-silica mixed oxides and this review summarizes most of that collective work.[9−11] Selected contributions from other laboratories will be discussed in light of these results.

The discovery of Ti-substituted silicalite molecular sieve, TS-1, as a catalyst for selective oxidation reactions with aqueous hydrogen peroxide[12] was quite exciting since water is detrimental to conventional titania-silica catalysts and no environmentally undesirable side products are formed from hydrogen peroxide reactions. However, the small size of the pores restricts the use of TS-1 to reactions involving small molecules. Thus, there is continuing interest in the synthesis of catalysts with larger pore sizes in order to accommodate bulkier molecules of importance for the production of fine chemicals. Since an excellent review of crystalline titanosilicate molecular sieves has been published recently,[13] we have not included a detailed discussion of these materials. Instead, the physical and chemical properties of TS-1 and analogous materials are compared to those of amorphous titania-silica mixed oxides when appropriate.

II. Synthesis of Ti−Si Mixed Oxides

The unique chemical and physical properties exhibited by titania-silica binary oxides depend on both the composition and the degree of homogeneity. Therefore, strategies have been developed to synthesize the mixed oxides in a uniform manner and typically include coprecipitation,[3,4,6] flame hydrolysis,[14] and sol−gel hydrolysis.[15,16] This review focuses on wet chemical techniques only. By precisely controlling hydrolysis conditions and drying procedures, high surface area aerogels and xerogels with a wide variety of compositions and pore structures can be synthesized.[17]

We have prepared a series of Ti−Si mixed oxides by simultaneous hydrolysis and condensation of metal alkoxides by controlling the rate of addition of water to a mixture of titanium isopropoxide and tetraethyl orthosilicate (TEOS) in 2-propanol.[9] The resulting coprecipitates were dried and subsequently calcined in flowing air to give high surface area, microporous mixed oxides. Micropores in these cohydrolyzed samples ranged from 1 to 1.5 nm in diameter as determined from the MP method. A summary of the compositions and surface areas of the samples is presented in Table 1. The microporous samples are denoted by their Ti:Si atomic ratio throughout this review. Klein et al. have prepared a similar set of mixed oxides by a sol−gel route.[18] In their study, hydrochloric acid was added to the alkoxide solutions to catalyze the sol−gel process. Calcination of their materials resulted in microporous mixed oxides with pores ranging from 0.6 to 0.8 nm in diameter.

An important problem associated with sol−gel synthesis is the unequal hydrolysis rates of the precursor

* To whom correspondence should be addressed.
† Current address: School of Chemical Engineering, Purdue University, West Lafayette, IN 47907.
⊗ Abstract published in *Advance ACS Abstracts,* August 15, 1997.

S0897-4756(97)00314-1 CCC: $14.00

Table 1. Surface Areas and Elemental Compositions of Titania−Silicas[9,11]

sample	Ti:Si atomic ratio	surface area/m^2 g^{-1}
TiO_2		100
Ti:Si 6:1	5.72:1	310
Ti:Si 1:1	1:1.08	450
Ti:Si 1:8	1:8.20	410
meso-TiSi−40[a]	1:49	1052
meso-TiSi−20[a]	1:66	1051
SiO_2		390

[a] Dilute titania in MCM-41 type mesoporous silica. The numerical values 40 and 20 refer to the nominal pore sizes associated with different surfactants used during synthesis.

metal alkoxides. Alkoxides of Ti, e.g., isopropoxide or butoxide, are typically hydrolyzed in water much faster than the standard Si alkoxide, tetraethyl orthosilicate, so separate titania-rich phases may form during synthesis. This problem can be mitigated by prehydrolyzing the TEOS before adding the titanium alkoxide[15,19] and by controlling the acidity/basicity of the medium.[15] Miller et al. compared directly the effects of prehydrolyzing the TEOS with small amounts of water and nitric acid before adding titanium butoxide.[20] Removal of the alcohol solvent was accomplished by extraction with supercritical carbon dioxide. Evidence from their characterization methods indicated that prehydrolysis of TEOS results in better atomic-level mixing of the Ti and Si components. They suggested that silica-rich patches can cover titania-rich cores when the mixed oxides are prepared without prehydrolysis of the TEOS. Dutoit et al. adjusted the reactivity of the Ti alkoxide by modifying titanium isopropoxide with acetylacetone.[21] This modified Ti precursor was then cohydrolyzed with tetramethyl orthosilicate in the presence of alcohol, water, and hydrochloric acid. Again, characterization results of the dried materials verified that excellent atomic-level mixing can be accomplished with this synthesis method.

A rather innovative synthetic method for producing well-mixed titania-silica was reported recently by Miller et al.[22] They chose to use diethoxysiloxane−ethyltitanate copolymer as a cation source since the Ti−O−Si linkage is already present in the precursor. After gelation, supercritical drying and calcination, the resulting titania-silica sample (6.25% titania) had a specific surface area of 840 m^2 g^{-1} and a pore volume of 3.0 cm^3 g^{-1}. Preliminary characterization experiments suggested that the Ti−O−Si linkages were preserved in the final product. This synthetic route avoids the problems associated with unequal hydrolysis rates of metal alkoxide precursors often used to prepare mixed oxide catalysts.

Drying conditions can profoundly influence the resulting porosity and homogeneity of titania-silica mixed oxides. Dutoit et al. directly compared the effects of conventional drying, high-temperature supercritical drying, and low-temperature semicontinuous supercritical extraction with carbon dioxide on the properties of Si-rich titania-silica.[21] Conventionally dried materials, or xerogels, were mostly microporous and had excellent dispersion of titania into silica. High-temperature supercritical drying of the samples formed meso- and macroporous materials, called aerogels, that partially segregated to form anatase titania. The aerogels formed by low-temperature extraction of solvent with supercritical carbon dioxide showed excellent atomic level mixing of components and very high surface areas. However, some microporosity was formed by this method.

Uniformly mesoporous, Si-rich mixed oxides can also be synthesized by procedures similar to those used for preparing MCM-41 mesoporous silicas,[23] but including a titanium source in the synthesis mixture. Corma et al. used IR spectroscopy, X-ray diffraction, UV spectroscopy, and catalytic testing to show that Ti from an ethoxide precursor incorporates into an MCM-41 silica templated by quarternary ammonium salts.[24] Similarly, Pinnavaia's group[25,26] and Gontier and Tuel[27] used alkylamines as the surfactants in the synthesis of mesoporous silica molecular sieves containing small amounts of titania. Our work in this area essentially follows the procedures outlined by Corma et al.[11] For example, a surfactant like hexadecyltrimethylammonium chloride is first combined with an ammonium hydroxide solution. In a separate flask, tetramethylammonium hydroxide is added to a solution of tetramethylammonium silicate. After the two mixtures are combined, fumed silica is added. Finally, titanium ethoxide is added dropwise under stirring to produce a synthesis gel with a nominal loading of 2 mol % Ti. After aging, the solids are filtered, washed, and calcined in flowing air. The isotherms for these mesoporous mixed oxides are similar to those reported previously for MCM-41 type materials.[25,28] Table 1 contains entries for two mesoporous Ti−Si mixed oxides, meso-TiSi-20 and meso-TiSi-40. They were prepared with two different sized surfactant molecules in order to give materials with nominal pore sizes of 20 and 40 Å, respectively.

A novel postsynthetic modification of mesoporous silica (MCM-41) with a Ti metallocene complex results in extremely high dispersion of Ti atoms on the surfaces of silica.[29] The intriguing aspect of this material is that all of the Ti atoms are isolated surface atoms. Apparently, the metallocene precursor prevents the formation of oligomeric titano−oxo species that lead to a separate titania phase, which is commonly observed with methods employing Ti chlorides or alkoxides.

III. Structural Evaluation of the Materials

A necessary first step in materials characterization is the determination of bulk structure. Even though catalysis is a surface phenomenon, insights derived from bulk analysis of solid catalysts often prove to be very useful. Indeed, many of the titania−silica materials discussed in the literature have extremely high surface areas, thus exposing a significant fraction of their atoms. In those cases, bulk analyses may provide some direct evidence for surface structures that may be important for catalysis.

An obvious tool for bulk structural characterization of titania-silicas is X-ray diffraction. However, in most cases, these materials are highly disordered and X-ray amorphous. Therefore, techniques that probe local structure around nearest-neighbor and next-nearest-neighbor atoms are the most effective. Spectroscopic tools have been applied with great success to the titania-silica system. These techniques include X-ray, ultraviolet, infrared, and nuclear magnetic resonance spectroscopies. Each technique provides unique and complementary information that can be combined to provide a fairly complete description of the solids.

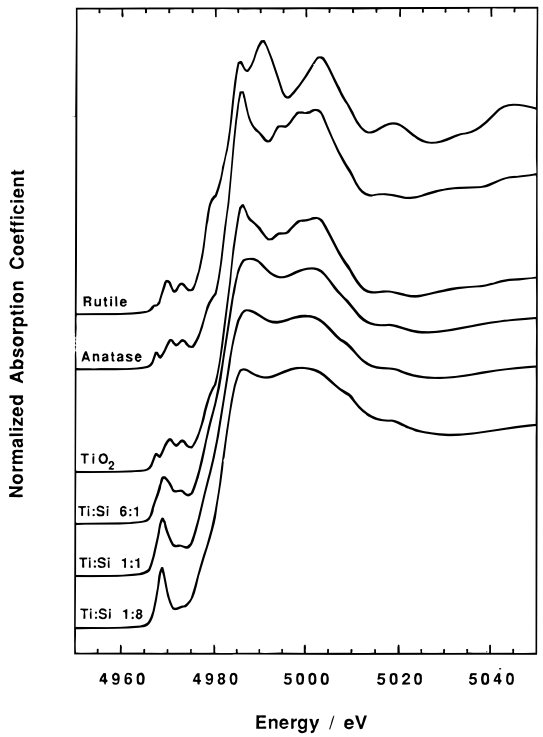

Figure 1. Ti K edge XANES for Ti oxides and Ti−Si mixed oxides. Reprinted with permission from ref 9.

Results from each technique applied to titania-silica will be discussed separately below.

X-ray Absorption Spectroscopy. *1. X-ray Absorption Near-Edge Structure (XANES).* The easy accessibility of the Ti metal K edge (4966 eV) at most synchrotron radiation facilities makes X-ray absorption spectroscopy an ideal method for probing local structure around the Ti component of the mixed oxide catalysts. The X-ray absorption near-edge spectrum at the Ti K edge contains several well-defined preedge peaks that are related to the local structure surrounding Ti. After studying a wide range of Ti-containing minerals, Waychunus concluded that it may be possible to arrive at the Ti site symmetry solely from the near-edge structure.[30] In Figure 1, crystalline titanias, anatase, and rutile exhibit three small preedge peaks, which are assigned to transitions (in order of increasing energy) from the 1s core level of Ti to $1t_{1g}$, $2t_{2g}$, and $3e_g$ molecular orbitals.[14] The intensities of these preedge features are a strong function of the distortion of the oxygen octahedron around the central absorbing Ti atom. For example, the variation in Ti−O bond distances is greater in rutile than in anatase, which distorts the regular octahedral coordination of Ti, resulting in slightly more intense preedge features for rutile. On the other hand, tetrahedrally coordinated Ti materials exhibit a single, intense, preedge peak since a regular tetrahedron lacks an inversion center.[14] Therefore, the relative intensities of the preedge features can be a sensitive measure of the local coordination environment around an average Ti atom. Unfortunately, a 5-coordinated titanium material such as fresnoite also exhibits a strong preedge feature, thus complicating the interpretation. Therefore, conclusions derived from analysis of the preedge region must be corroborated by evidence from additional techniques.

The near-edge spectra associated with Ti−Si mixed oxides prepared in our laboratory are compared to those of anatase and rutile in Figure 1. The formation of anatase is indicated by the near edge region of TiO_2 prepared by hydrolysis of Ti alkoxide, and X-ray diffraction of this sample revealed broad lines at diffraction angles corresponding to anatase with no evidence of rutile formation. As silicon is incorporated into the mixed oxides, a single preedge feature begins to dominate the other weaker features. For example, little structure is present in the preedge region of Ti:Si 1:8 except for a single preedge peak.

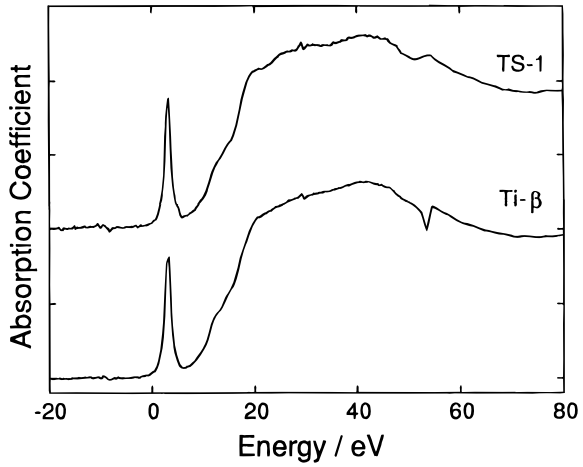

Figure 2. Ti K edge XANES for TS-1 and Ti-β molecular sieves. All energies are referenced the first inflection point in the Ti foil K edge [adapted from ref 31].

At low Ti contents, Ti may substitute directly for Si in the tetrahedral SiO_2 framework. Figure 2 shows the analogous near edge spectra for TS-1 and Ti-β, molecular sieves in which Ti atoms partially replace Si atoms in regular tetrahedral framework sites.[31] Clearly, the preedge peaks for the mixed oxides are not as intense as that expected for Ti in a completely tetrahedral environment, but instead are consistent with the presence of either 5-coordinated Ti or mixtures of 4-, 5-, and 6-coordinated Ti.

Since the specific surface areas of Ti−Si mixed oxides are often very high, a significant fraction of the Ti atoms may be exposed to the surface. Therefore, in situ dehydration of the samples may reveal a substantial change in coordination as detected by XANES. Figure 3 illustrates the effect of removing water from the surfaces of a mixed oxide that is fairly dilute in Ti. The large preedge feature in the dried sample indicates that the majority of Ti occupies sites of tetrahedral symmetry, as expected for samples in which Ti substitutes directly for Si in the mixed oxide. Apparently, adsorbed water disrupts the regular tetrahedral geometry associated with the dehydrated sample. No change was seen in the preedge region of a titanium-rich sample after dehydration, presumably because most Ti atoms reside in bulklike octahedral sites.

The extent of reduction of Ti^{4+} to Ti^{3+} can be assessed from the positions of the preedge peaks. A comparison of the XANES for compounds containing either Ti^{3+} or Ti^{4+} reveals an average shift of 2.0 eV to higher energies for features associated with Ti^{4+} compounds relative to Ti^{3+} compounds.[30] In our work, we found no significant shifts in spectral features to indicate the presence of Ti^{3+}. Most of the Ti in those samples remained in the 4+ oxidation state, which is consistent with earlier work on Ti-substituted silica glasses.[14]

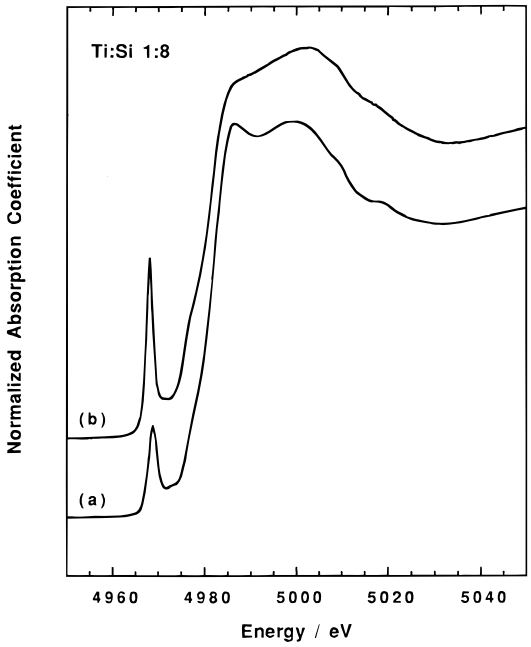

Figure 3. Effect of dehydration on the Ti K edge XANES in Ti:Si 1:8 mixed oxide: (a) sample in ambient air; (b) sample dehydrated at 573 K for 3 h in flowing He. Reprinted with permission from ref 9.

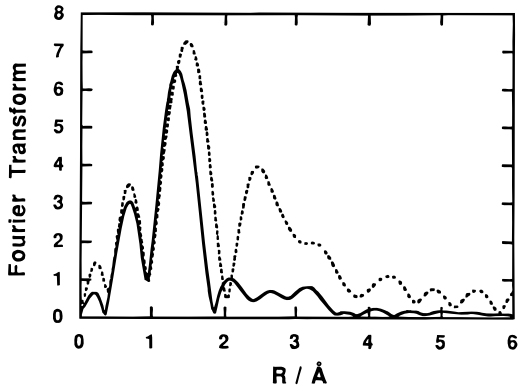

Figure 4. Comparison of radial structure functions not corrected for phase shifts (a), and Fourier filtered EXAFS functions (b), for Ti:Si 1:8 (solid lines) and synthesized TiO_2 (dotted lines). Reprinted with permission from ref 9.

Table 2. Effect of Composition on Ti−O Interatomic Distances Derived from the Ti K Edge EXAFS of Ti−Si Mixed Oxides[9]

sample	Ti/Ti + Si	*R*/Å
TiO_2	1	1.94
Ti:Si 6:1	0.85	1.91
Ti:Si 1:1	0.48	1.88
Ti:Si 1:8	0.11	1.82
meso-TiSi−20	0.015	1.79

As mentioned above, the coordination environment of Ti cannot be unambiguously determined solely from the intensity of the preedge peak since 5-coordinated Ti can also produce a significant preedge feature. However, attributing the preedge feature in Figure 3b to tetrahedrally coordinated Ti is justified by results from other techniques that will be discussed later. Greegor et al. studied a series of TiO_2-SiO_2 glasses containing very low levels of Ti by X-ray absorption spectroscopy and correlated the fraction of Ti atoms occupying tetrahedral environments with preedge peak area.[14] Comparison of their spectra with Figure 3b reveals that approximately 70% of the Ti atoms in dehydrated Ti:Si 1:8 reside in tetrahedral sites.

2. Extended X-ray Absorption Fine Structure (EXAFS). The EXAFS region of the X-ray absorption spectrum provides complementary structural information on the local environment surrounding Ti. A Fourier transform of the EXAFS data gives a radial structure function, RSF, surrounding an average Ti atom. Since the reported RSF is often not corrected for phase shifts, the actual values of interatomic distances are calculated from curve fits to standard materials. Figure 4 compares the RSF of TiO_2 with that of Ti atoms diluted in silica. The large peak in the radial structure functions indicates the Ti−O first-nearest-neighbor coordination shell. Shortening of the average Ti−O bond distance in the mixed oxide is readily apparent from a comparison of the radial structure functions of TiO_2 and Ti:Si 1:8 shown in Figure 4. Anatase titania has a known average Ti−O bond distance of 1.95 Å. Curve fitting of the EXAFS results in Figure 4 provide an interatomic distance of 1.82 Å for Ti atoms diluted in silica,[9] which compares favorably with 1.80 Å for tetrahedrally coordinated Ti in titanium silicalite molecular sieve,[32] 1.81 Å for Ti substituted in Al-free zeolite β,[31] and 1.79−1.84 Å for Ti in doped silica glasses.[14,33,34] Sandstrom et al. investigated the variation in metal−oxygen bond distances as a function of 4- and 6-fold coordination in Ti and Ge materials and discovered that a short bond distance (1.82 Å for Ti−O) corresponds with the cation residing in a tetrahedral environment.[33] In a separate study, Pei et al. compiled a list of the average Ti−O interatomic distances in compounds with titanium in various states of coordination.[32] The average bond distance in compounds with Ti in 6-fold coordination is about 1.96 ± 0.01 Å, excluding $MgTiO_3$ which presents an anomalously short average distance of 1.85 Å. The average Ti−O bond distance in 5-coordinated fresnoite is 1.92 Å, whereas the average bond distance of 4-coordinated compounds is 1.79 ± 0.02 Å.[32] Neurock and Manzer used density functional methods to calculate a Ti−O bond distance of 1.81 Å in a tetrahedral cluster.[35] Clearly, the value of 1.82 Å reported for the Ti−O bond distance in Ti:Si 1:8 mixed oxide is consistent with a majority of the Ti atoms residing in a tetrahedral environment, which corroborates the similar conclusion from XANES. As shown in Table 2, a fairly linear variation in Ti−O bond distance with titanium content is observed. As the titanium content decreases, the average first-shell interatomic distance changes from 1.94 to 1.82 Å. A very dilute sample of Ti substituted into mesoporous MCM-41 silica (meso-TiSi-20 in Table 2) also exhibits a short Ti−O bond distance, consistent with isomorphous substitution of Ti atoms into tetrahedral sites.[11]

The higher shell peaks appearing between 2 and 4 Å in the RSF of TiO_2 (Figure 4) are absent in the mixed oxide. Schultz et al. attributed the lack of higher shells in the RSF of Ti-substituted ZSM-5 to a large distortion of the structure near the Ti sites.[36] The lack of large higher shell peaks is also expected if Si atoms replace Ti atoms in the second coordination shell; silicon backscatters the photoelectron wave less effectively than higher Z elements such as Ti.

The combined results from XANES and EXAFS provide valuable information on the local environment around Ti in the mixed oxides. The experiments show

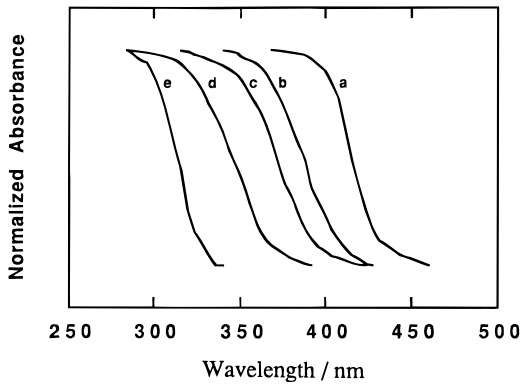

Figure 5. Normalized absorption spectra derived from UV diffuse reflectance spectroscopy of (a) rutile, (b) Ti:Si 6:1, (c) Ti:Si 1:1, (d) Ti:Si 1:8, and (e) Ti:Si 1:8 dehydrated in vacuum at 523 K for 5 h. Reprinted with permission from ref 9.

convincingly that, in Ti-rich mixed oxides, coordination of Ti atoms is octahedral, similar to the bonding in pure titania. In Si-rich oxides, the coordination of Ti atoms is mostly tetrahedral, similar to the bonding in Ti-substituted molecular sieves. The coordination environments around Ti atoms in oxides of intermediate compositions cannot be determined from these methods but most likely consist of mixtures of 4-, 5-, and 6-fold sites.

Ultraviolet Diffuse Reflectance Spectroscopy. Results from X-ray absorption spectroscopy verified that the oxides were indeed mixed at the molecular level since the coordination environment of Ti is dramatically affected by elemental composition. However, complete isolation of the Ti atoms cannot be achieved throughout the composition range. Thus, small domains of titania or Ti-rich mixed oxides must be present in some of the materials.

Ultraviolet spectroscopy has been utilized to characterize the bulk structure of crystalline and amorphous titania-silicas.[37] Titania is a semiconductor oxide with an easily measured optical bandgap. Ultraviolet diffuse reflectance spectroscopy is used to probe the band structure, or molecular energy levels, in the materials since UV excitation creates photogenerated electrons and holes. The UV absorption threshold is a strong function of titania cluster size for diameters less than 10 nm, which can be attributed to the well-known quantum size effect for semiconductors.[38] Our group has previously used the quantum size effect to approximate the average crystallite size of titania clusters supported on VPI-5 molecular sieve,[39] and the same reasoning can be used to estimate the size of titania-like domains in Ti−Si mixed oxides.

Normalized absorption spectra derived from UV reflectance data are presented for representative titania-silica samples in Figure 5. The position of the absorption edge for rutile corresponds to its known bandgap energy of 3.0 eV (410 nm). The UV absorption edge for the Ti:Si 6:1 sample overlaps the spectrum of pure anatase (not shown), which is shifted by about 30 nm from rutile to 380 nm. As the content of Si in the mixed oxides increases, the UV absorption edge shifts to higher energies. The absorption edge in the most Si-rich mixed oxide, Ti:Si 1:8, is blue-shifted by about 45 nm relative to the edge in the most Ti-rich mixed oxide, Ti:Si 6:1.

Earlier results from UV absorption spectroscopy of a titanosilicate molecular sieve revealed an absorption peak at 212 nm with the midpoint of the absorption edge at 260 nm.[40] In that material, Ti substitutes directly for Si in the SiO_4^{4-} tetrahedra, and the concentration of Ti is so low that virtually no Ti−O−Ti linkages are present. Therefore, the observed UV absorption peak is attributed to molecular excitations of isolated TiO_4^{4-} units instead of excitations within the fully developed titania band structure. Results from UV reflectance spectroscopy of 2 wt % titania in mesoporous silica overlap those of TS-1 indicating that, at very low weight percents, Ti atoms can reside in an amorphous silica matrix with few or no Ti−O−Ti linkages.[11]

In the spectrum of Ti:Si 1:8 (dehydrated), the absorption edge was about 50 nm greater than the absorption edge in titanosilicate molecular sieves, indicating that small microdomains of titania must exist in the sample. Using the hyperbolic band model of Wang et al.[41] for spherical particles and assuming that the effective masses of the photogenerated hole and electrons are $m_h^* = 3m_e$ and $m_e^* = 20m_e$, respectively (m_e is electron mass),[42,43] we estimate the titanium oxide domain in the dehydrated Ti:Si 1:8 sample is 1 nm (10 Å) in diameter. This calculation is based on the blue-shift of the UV absorption edge in Figure 5e from the bulk phase rutile spectrum in Figure 5a. Since the coordination environments and interatomic distances of the Ti microdomains in Ti:Si 1:8 are fundamentally different from rutile (and anatase), the calculation of domain size based on a quantum size effect relative to rutile is only a rough approximation at best.

Most of the Ti atoms in the small domain of a silica-rich sample must form Ti−O−Si linkages rather than Ti−O−Ti linkages, which is consistent with the results from X-ray absorption spectroscopy. The Ti domains grow progressively larger with increasing Ti content in the mixed oxides which is indicated by the shift of the absorption edges to longer wavelengths.

Vibrational Spectroscopy. Techniques such as X-ray and UV spectroscopies are useful for determining electronic and atomic structural information of mixed oxides. However, longer wavelength spectroscopies reveal how atomic-level mixing of titania and silica perturbs the normal vibrational modes of the solids.

1. Laser Raman Spectroscopy. The laser Raman spectra of anatase, rutile, and some representative mixed oxides are shown in Figure 6. The mixed oxides reveal three main features that appear in regions associated with both anatase and rutile and two peaks that appear at very low wavenumbers (310 and 238 cm^{-1}). In addition, the titania bands in the mixed oxides are much broader and are shifted from the peak positions of the reference materials. Since no Raman peaks were observed in either Ti:Si 1:8 or pure silica, all of the peaks shown in Figure 6 were attributed to the Ti component of the mixed oxide.

The Raman feature at 640−650 cm^{-1} is present in most of the mixed oxide samples but decreases in intensity relative to the 430 cm^{-1} peak with decreasing Ti content. The same decrease in relative intensity is also observed for the band at 530−540 cm^{-1}, and both bands appear to be broadened peaks of anatase shifted to greater wavenumbers by 10−20 cm^{-1}. The band at 430−440 cm^{-1} becomes the dominant band as the Si

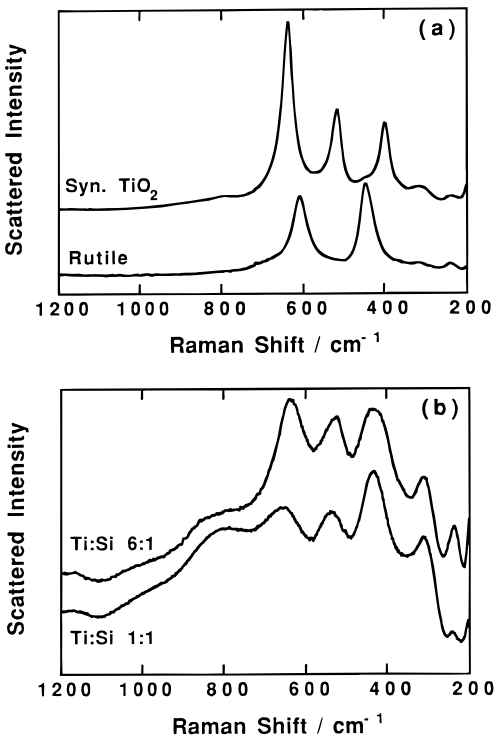

Figure 6. Laser Raman spectra of (a) pure titanium dioxides and (b) Ti−Si mixed oxides. Reprinted with permission from ref 9.

content increases and is the only band (although very weak) in the Ti:Si 1:5 sample. The 430−440 cm^{-1} band could be either a rutile peak shifted by about 10 cm^{-1} to lower wavenumbers or an anatase peak shifted by about 30 cm^{-1} to greater wavenumbers. However, even though we favor assignment of this peak to an anatase-like domain, we could not confidently attribute the 430−440 cm^{-1} feature to either crystal phase. Previous Raman studies of Ti−Si mixed oxides have attributed this band to Si−O−Si and O−Si−O bending vibrations,[15,19] but that assignment is inconsistent with the fact that the peak is fairly intense in Ti-rich samples.

The same set of peaks has been observed for nanophase titania clusters supported inside the channels of VPI-5 molecular sieve, but in that study the 430 cm^{-1} band was attributed to the molecular sieve.[39] The broadening and shifting of the anatase peaks at 540 and 670 cm^{-1} in the supported nanophase titania clusters were attributed to a deficiency of oxygen in the clusters. Raman spectroscopy of nanophase TiO_2 clusters, prepared by gas-phase condensation and oxidation of Ti, revealed that peaks are broadened and shifted by 10−20 cm^{-1} upon removal of a small amount of oxygen to give $TiO_{1.88}$.[44,45] Since the incorporation of Si in the Ti−Si mixed oxides greatly disturbs the octahedral coordination environment of Ti, it is reasonable to postulate that the Raman shifts observed in this work result from small changes in the average oxygen content in the titania microdomains. Another plausible explanation can also be proposed.[9] Arashi has studied the effects of applied pressure on the Raman spectrum of rutile and found that the peak positions at 446 and 608 cm^{-1} increase linearly with pressure up to about 500 and 660 cm^{-1}, respectively, at 10 GPa.[46] The shortening of the average Ti−O bond distance in the mixed oxides may have the same effect on the solid vibrational modes as

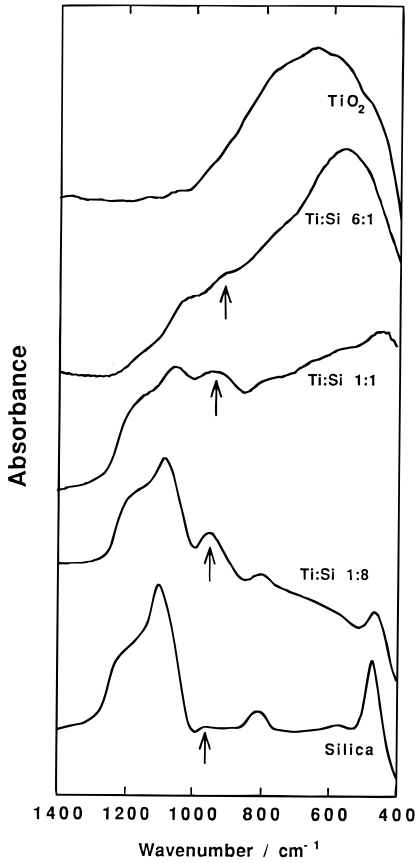

Figure 7. FT-IR absorption spectra of Ti−Si mixed oxides. Reprinted with permission from ref 9.

applied pressure and thus could account for the shift in the anatase-like bands upward compared to the pure oxide.

The low wavenumber peaks in the mixed oxide at 310 and 238 cm^{-1} have been assigned by Schraml-Marth et al.[15] as titania lattice modes that become Raman active only after crystallite dimensions are reduced to less than 30 nm, which is consistent with the small size of the titania domains in the samples determined from the shifts in the UV absorption spectra. In addition, by studying nanophase titania particles, Melendres et al. found that a 240 cm^{-1} band present in some rutile preparations is likely due to a second-order scattering process or latent anharmonicity.[47]

2. Infrared Absorption Spectroscopy. The low-wavenumber region of the IR absorption spectrum has been used extensively to characterize Ti−Si mixed oxides and Ti-substituted molecular sieves. Example spectra of Ti−Si mixed oxides are given in Figure 7. The silica-rich sample, Ti:Si 1:8, exhibits the symmetric stretching vibration band at 807 cm^{-1} and the asymmetric vibration band at 1090 cm^{-1} of the tetrahedral SiO_4^{4-} structural unit. The broad absorption feature for Ti:Si 6:1 centered at about 550 cm^{-1} is representative of titanium dioxide. An additional feature, depicted with arrows in Figure 7, appears with the greatest intensity in Ti:Si 1:8. The position of this band is ∼935 cm^{-1} in the 1:1 sample and ∼955 cm^{-1} in the 1:8 sample. The pure silica sample has a very small peak in this region, which is assigned to the stretching vibration of free silanol groups at the surface.[15] A large increase in the relative peak intensity of the ∼960 cm^{-1} band is seen in the 1:8 sample and is often used as evidence for Ti

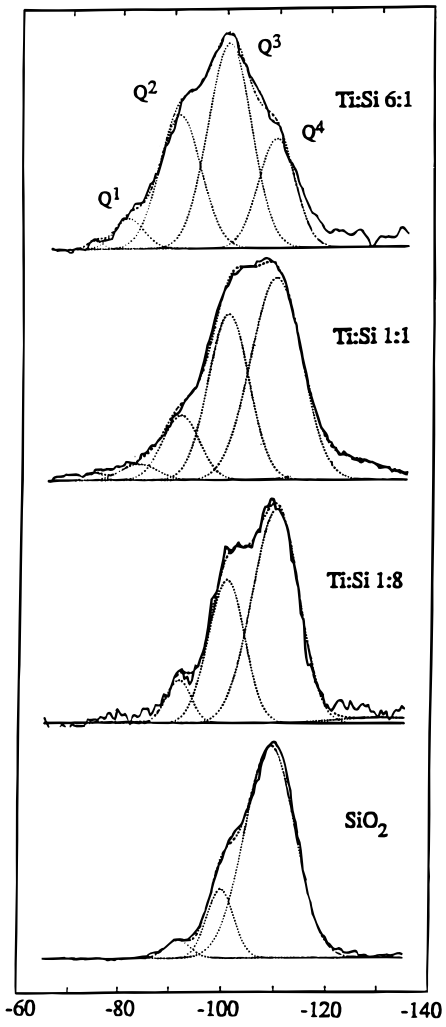

Figure 8. ^{29}Si single-pulse MAS NMR spectra with peak deconvolution and curve fitting (dotted line) for pure silica and microporous Ti−Si mixed oxides.[11]

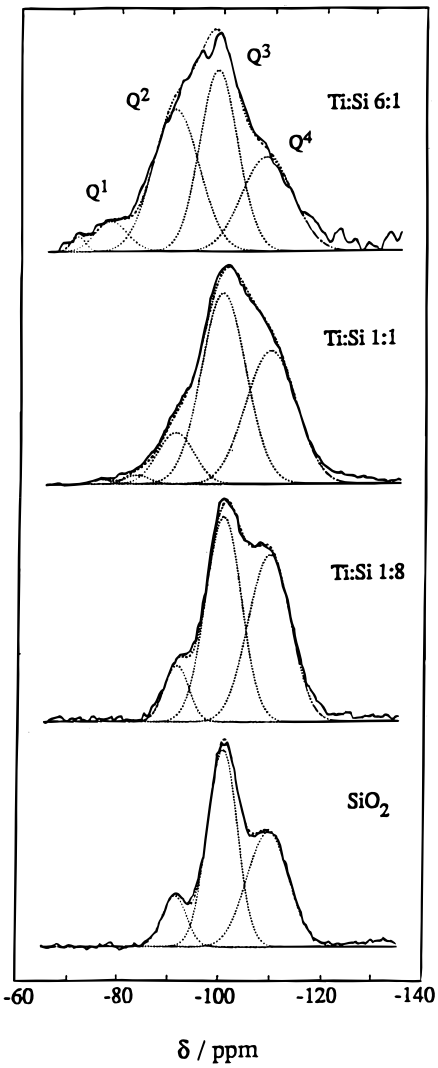

Figure 9. ^{1}H−^{29}Si cross-polarization MAS NMR spectra with peak deconvolution and curve fitting (dotted line) for pure silica and microporous Ti−Si mixed oxides.[11]

incorporation into the silica lattice. Indeed, some researchers have used this band to quantitatively assess the degree of Ti−O−Si heterolinkages in titania-silica samples.[21] However, pure silica can have a significant IR absorption band in this region.[48] Since the 960 cm^{-1} band results from both Ti−O−Si and Si−O^{-} contributions, use of this band for quantitative analysis is questionable.

^{29}Si MAS NMR Spectroscopy. The results from X-ray, UV, and Raman spectroscopies provided information on the local structure of the Ti component of the binary oxides. Infrared spectroscopy was the only bulk technique discussed so far that provided some insights into the effect of mixed oxide formation on the characteristics around Si atoms. The best tool for elucidating the connectivity of silicon atoms in solid oxide materials is probably silicon NMR spectroscopy.

Figures 8 and 9 show the ^{29}Si single pulse (SP) and ^{1}H−^{29}Si cross-polarization (CP) solid-state MAS NMR spectra with peak deconvolution and curve fitting for pure silica and microporous Ti−Si mixed oxides. The SP SiO_2 spectrum clearly exhibits three well-resolved Gaussian peaks at chemical shifts of −109.2, −99.8, and −91.7 ppm, which can be assigned to Q^4 [$Si(SiO)_4$], Q^3 [$Si(SiO)_3(OH)$], and Q^2 [$Si(SiO)_2(OH)_2$] structural units, respectively.[49] The relative amounts of these different structural sites are derived from the integrated areas of the single pulse peaks. As Figure 8 shows, Q^4 sites are dominant in pure silica, indicating that the sample has a well-developed three-dimensional framework. About 19% of the Si nuclei are directly bonded to hydroxyl groups, which is consistent with the enhancement of the Q^3 and Q^2 signals relative to Q^4 under the CP condition. Previous work on silica gels and silicates has shown that the most likely candidates for ^{1}H−^{29}Si cross polarization are hydrogens in SiOH groups,[49,50] even though the hydrogens of adsorbed water could contribute to the enhancement under certain conditions. The spectra of Ti:Si 1:8 exhibit features similar to those of the synthesized silica, as shown in Figures 8 and 9. However, the relative number of Q^4 sites decreased, while Q^3 and Q^2 sites increased. Walther et al. also observed similar features in their study of mixed oxides.[16] As silica was chemically mixed with titania, the three-dimensional framework of silica, and the microstructure surrounding the silicon atoms, were significantly perturbed by Ti atoms. However, care must be exercised when discussing the effect of Ti on the spectrum. After studying the ternary silicate glass SiO_2−TiO_2−ZrO_2, Wies et al. found that −OH and −OTi groups have a similar influence on the chemical shift

of the central Si atoms,[51] which complicates the interpretation of the spectrum. This problem can be circumvented by comparing both the single pulse and cross-polarized spectra of the Ti−Si mixed oxides with those of the pure silica. As shown in Figure 8, the amounts of Q^3 and Q^2 groups increase with increasing Ti content. If the only non-Si atoms in the Q^3 and Q^2 groups were H atoms, then the signals for these groups in the spectra of the mixed oxides would be enhanced by the $^1H-^{29}Si$ CP procedure in a similar manner as pure silica. Instead, as a comparison of Figures 8 and 9 indicates, the enhancement factors for the intensities of the Q^3 and Q^2 sites of the spectra of the mixed oxides are much less than those for the silica. Therefore, H atoms are not the only non-Si atoms in the Q^3 and Q^2 in the mixed oxides. Evidently, some Si atoms in the second shell were replaced by Ti atoms, indicating that Si−O−Ti bonds were generated upon the chemical mixing. This finding is completely consistent with structural studies on these materials described above.

Summary of Results from Bulk Characterization. A consistent picture of the bulk structure of amorphous Ti−Si mixed oxide materials emerges from the combined results of all the techniques. Wet chemistry synthesis from alkoxide precursors produces well-mixed binary oxides. As the silicon content of the mixed oxide increases, the titania domain size decreases and the average Ti−O bond distance shortens, indicating that many of the Ti atoms change from octahedral coordination to tetrahedral coordination. However, the Ti atoms may not be completely isolated in the silica-rich mixed oxides but likely exist in small microdomains with some Ti−O−Ti linkages. At very low concentrations, Ti atoms in silica appear to be well-isolated and tetrahedrally coordinated like the Ti atoms in TS-1 molecular sieve.

IV. Surface Characterization

Characterization of the mixed oxide surface is necessary for understanding catalysis over these materials. Unfortunately, observed surface features are often unrelated to active catalytic sites, since these sites may occupy only a small fraction of the surface and many characterization techniques are not capable of interrogating surfaces under reaction conditions. Modern electron spectroscopies have provided a wealth of fundamental information on the surface structure of metals and single-component metal oxides. However, the high porosity and complex nature of many mixed oxides hinder the application of standard surface science techniques. In the next section, results from spectroscopic and temperature-programmed methods will be used to derive information on the nature of titania-silica mixed oxide surfaces.

X-ray Photoelectron Spectroscopy. Information on the surface composition and electronic structure of mixed oxide components can be derived from X-ray photoelectron spectroscopy. A recent XPS study of titania-silica mixed oxides revealed that Si is preferentially located at the surfaces of Ti-rich mixed oxides, which may account for their relatively high surface areas.[52] Indeed, the tripling of surface area upon silica incorporation into titania (shown in Table 1) supports the idea that silica preferentially locates at the surfaces of titania-rich mixed oxides and prevents sintering. A summary of the elemental compositions of Ti:Si mixed oxides determined from bulk analysis and XPS of our samples is presented in Table 3. Silicon clearly enriches the surfaces of the Ti-rich mixed oxide, which is consistent with previous studies.[52] Since Si cannot isomorphously substitute into the titania crystal structure, addition of small amounts of silica to titania creates a highly defective interface which results in a high surface area mixed oxide. The bulk and surface compositions of the Si-rich materials shown in Table 3 are the same. Apparently, isomorphous substitution of Ti for Si accounts for the excellent distribution of Ti throughout the sample.

Table 3. Comparison of Surface and Bulk Compositions of Ti:Si Mixed Oxides

sample	Ti/(Ti + Si) from XPS	Ti/(Ti + Si) from bulk analysis
Ti:Si 6:1	0.32	0.85
Ti:Si 1:1	0.35	0.48
Ti:Si 1:8	0.11	0.11
Ti:Si 1:18	0.049	0.051

The core level binding energies of the elements also provide insights into the degree of atomic level mixing. However, values of binding enegies should be reported and interpreted with great care. Since pure titania is a semiconductor whereas pure silica is an insulator, the degree of differential charging on small particles will be a function of composition. For highly siliceous materials such as TS-1, a common method for charge correction is to assign the Si 2p core line to that of pure silica and adjust the Ti core-level binding energies appropriately. Unfortunately, a constant binding energy for Si core levels cannot be assumed for Ti−Si mixed oxides that span the entire composition range. Another method for charge referencing involves the evaporation of small metal particles onto the oxide surfaces. Assuming that the metal particles charge identically to the support oxide during an XPS experiment, core levels of the supported metal may be used for charge correction. However, Schottky barrier effects may influence the observed energies. Carbon impurities resident on samples can also be used to assess the level of charging on insulator samples. Figures 10 and 11 show the effects of composition on the binding energies of Ti and Si 2p core levels. Sample charging was minimized with an electron flood gun, and charging effects were corrected for by assigning the C 1s peak to 284.5 eV.[53] As illustrated in Figures 10 and 11, the Ti 2p and Si 2p binding energies increase with addition of Si to the mixed oxides. The change in binding energy over the entire composition range is small (∼1.5 eV) but clearly discernible. Comparable core level shifts have also been reported for a series of Ti−Si mixed oxide photocatalysts.[37] Lassaletta et al. have studied titania samples by XPS using different sample preparation methods, including titanium evaporation in the presence of oxygen onto silica, oxidized silicon, or single-crystal graphite.[54] An increase in the Ti 2p binding energy by 0.7 eV was realized for small titania particles on silica compared to bulk titania, whereas no effect of particle size was found for titania on graphite. Thus, the titania-silica interface was speculated to be the most important parameter in those XPS experiments. Realizing that the binding energy shift is a combination of the initial state charge distribution and the extra-atomic relaxation of the photohole, Lassaletta et al. suggest

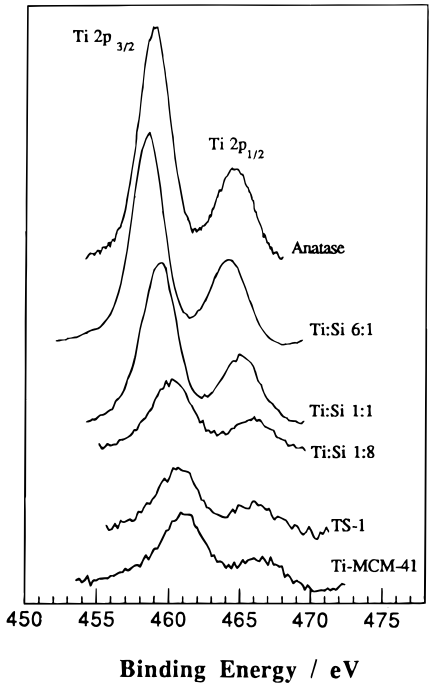

Figure 10. XPS of Ti 2p core levels of titania-silica mixed oxides.

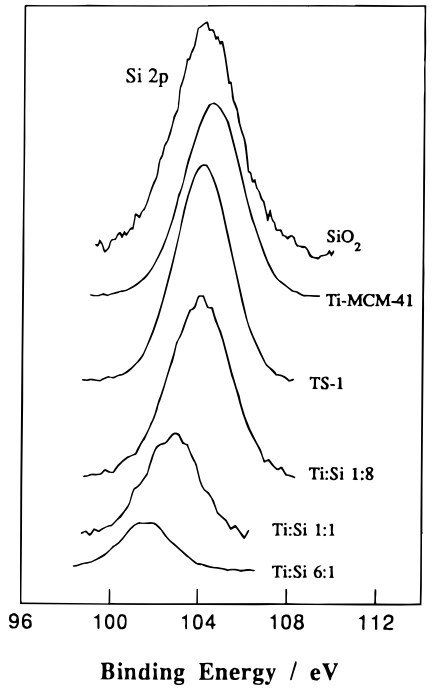

Figure 11. XPS of Si 2p core level of titania-silica mixed oxides.

that changes in the relaxation energy dominated the observed Ti 2p binding energy shift. If the oxygen atoms at the Ti−O−Si interface are less polarizable compared to those of bulk titania (which is expected based on the bulk dielectric constants of titania and silica), then the photoelectrons created by excitation of Ti at the titania-silica interface will be less effectively screened. The possible change of coordination environment around Ti from octahedral to tetrahedral at low Ti loadings should also affect the binding energies of the Ti core levels. Nevertheless, results from XPS of titania-silica mixed oxides shown in Figures 10 and 11 are consistent with a high degree of mixing near the surface regions of the samples, which is completely consistent with bulk phase characterization results.

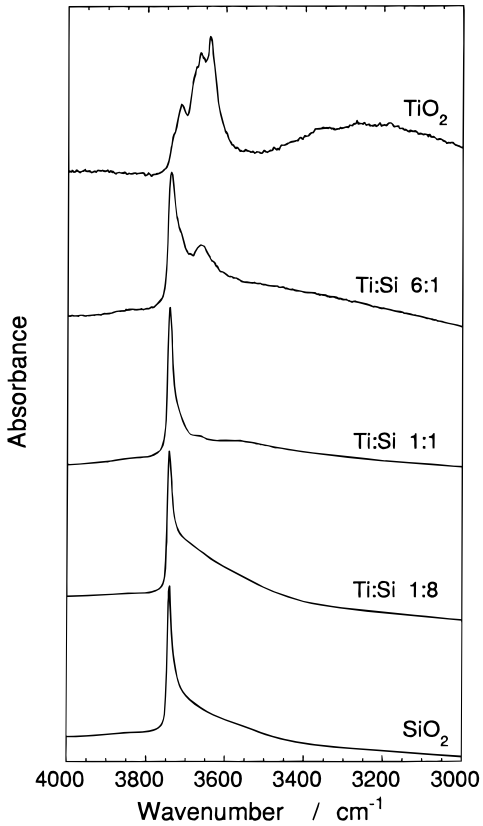

Figure 12. Hydroxyl region IR spectra of Ti−Si mixed oxide samples. All of the samples were treated in situ before acquisition of spectra.[10]

Infrared Spectroscopy. Infrared spectroscopy provided important information on the lattice vibrations of the mixed oxides as discussed earlier. Surface sensitive information can be derived from this technique if the surface O−H stretching region is examined and if molecular adsorbates are probed.

Pure silica and silica-rich Ti−Si mixed oxide exhibited a single, high wavenumber peak at 3740 cm^{-1} associated with isolated surface hydroxyl, or silanol, groups.[55] Pure titania and titania-rich mixed oxide revealed additional peaks at lower wavenumbers (3716, 3666, and 3640 cm^{-1}). These features are illustrated in Figure 12. Primet et al. observed multiple bands on anatase (3715, 3665 cm^{-1}) and on rutile (3685, 3655 cm^{-1}), and assigned the low-wavenumber band to hydrogen-bonded hydroxyl groups and the high-wavenumber band to isolated hydroxyl groups.[56] However, others have attributed the high-wavenumber band on titania to a silica impurity in the sample.[55,57]

The hydroxyl region for the mixed oxides is greatly perturbed by the adsorption of ammonia.[10] The spectrum for ammonia on titania exhibits broad bands at 3356 and 3280 cm^{-1} with shoulders at 3400 and 3190 cm^{-1}. The spectrum for Ti-rich mixed oxide has broad bands 3348, 3248, and 3183 cm^{-1}, whereas the spectrum for the silica-rich sample reveals only two well-defined bands at 3374 and 3285 cm^{-1}. Primet et al.[58] and Dines et al.[59] observed four bands in the NH stretching region of the IR spectrum of ammonia adsorbed on titania. They assigned the four bands to the symmetric and asymmetric stretches of ammonia adsorbed on two

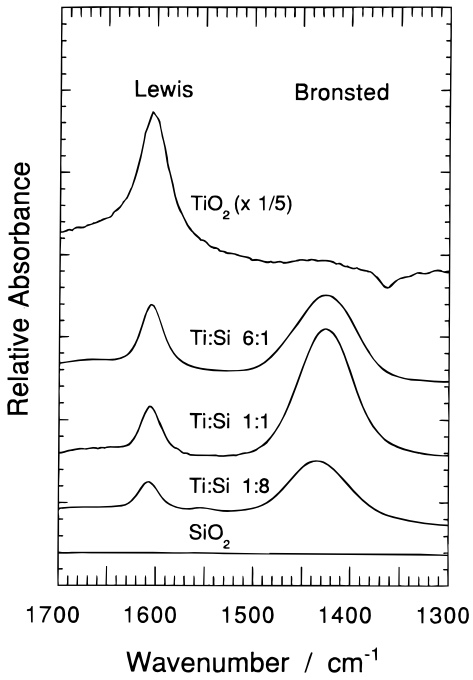

Figure 13. Low-wavenumber IR spectra of ammonia adsorbed on Ti−Si mixed oxides.[10]

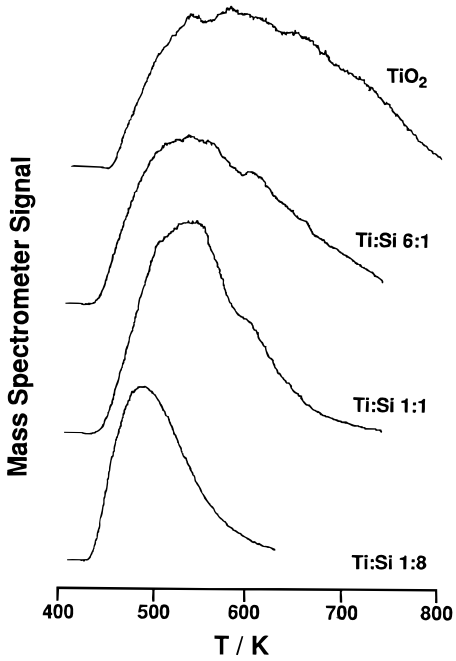

Figure 14. Results from temperature-programmed desorption of ammonia from titania and Ti−Si mixed oxides.[10]

different types of Lewis acid sites. Likewise, the multiple bands associated with titania and Ti-rich mixed oxides suggest that more than one type of Lewis acid site is present on the surfaces. Only a single type of Lewis acid interaction with ammonia is observed on our silica-rich mixed oxide.[10]

The low-wavenumber region from 1700 to 1300 cm^{-1} is useful for evaluating the number densities of Lewis and Bronsted acid sites on the mixed oxide surfaces. Figure 13 shows the two well-resolved peaks associated with ammonia adsorbed on a surface cation, or Lewis acid site (1605 cm^{-1}), and the ammonium ion resulting from adsorption on a Bronsted site (1430 cm^{-1}). The Bronsted peak areas cannot be directly compared to the Lewis peak areas without also considering the different extinction coefficients. The IR spectrum of ammonia on pure titania indicates that only Lewis acid sites are accessible for ammonia adsorption. Apparently, the hydroxyl groups on pure titania are not able to protonate ammonia under the conditions of that study. The large difference in the areas of the peaks at 1605 cm^{-1} for titania and Ti:Si 6:1 indicates that a relatively small amount of silica suppressed a major fraction of the Lewis acid sites normally associated with titania. These results are consistent with elemental compositions determined by XPS that indicate silica enrichment at the surface.

Desorption of ammonia at higher temperatures was also monitored by IR spectroscopy.[10] Almost no ammonia remained adsorbed on mixed oxide Lewis acid sites at 453 K, whereas about half of the ammonia remained on pure titania at the same temperature. These results suggest that ammonia is bound more strongly to the acid sites on pure titania than any of the mixed oxides. Quantitative information is derived from thermal desorption experiments.

Temperature-Programmed Desorption of Ammonia. The TPD of adsorbed ammonia can be used to estimate the density of acid sites on the mixed oxide surfaces.[10] Representative TPD curves are plotted in Figure 14. The highest density of acid sites was 3.2 × 10^{-6} mol m^{-2} for our pure titania, which compares to 5.8 × 10^{-6} mol m^{-2},[60] 1.5 × 10^{-6} mol m^{-2},[61] and 2.9−3.6 × 10^{-6} mol m^{-2} [62] determined in other laboratories by a variety of acid titration methods on titania. In our work, the number density of surface acid sites decreased with increasing silica content.[10] Nakabayashi[5] and Odenbrand et al.[60] also found lower surface acidities on the mixed oxides relative to titania. However, others have found the opposite result.[4,61,63] Evidently, no clear consensus exists to describe the trend in number density of surface acid sites on Ti−Si mixed oxides.

In addition to number density, the strength of the acid site plays an important role in catalysis. The ammonia TPD curves in Figure 14 most likely indicate that the strongest acid sites are present on pure titania and that acidity progressively weakens as Si is incorporated. However, ammonia TPD cannot be used to unambiguously rank materials according to acid strength because basic solids such as CaO can also adsorb ammonia quite strongly.[64] In addition, care must be exercised when interpreting TPD results from microporous materials since severe readsorption can occur during the experiment. However, the combination of ammonia IR spectroscopy and ammonia TPD on the same samples shows convincingly that the acid strengths of the mixed oxides decrease with increasing silica content. In contrast to our results, other researchers have observed strong acid sites on silica-rich samples.[3,4,60,61,63] Again, no clear consensus exists regarding the distribution of acid strengths on mixed oxides prepared in different laboratories.

Temperature-Programmed Reaction of 2-Propanol. The TPR of 2-propanol has been used previously to measure the titania surface areas of mixed oxides of titania and silica.[65] In that paper, however, titania was deposited onto a silica substrate and interfacial mixing was assumed to be minimal. Therefore, the samples of that study are very different from the nearly homoge-

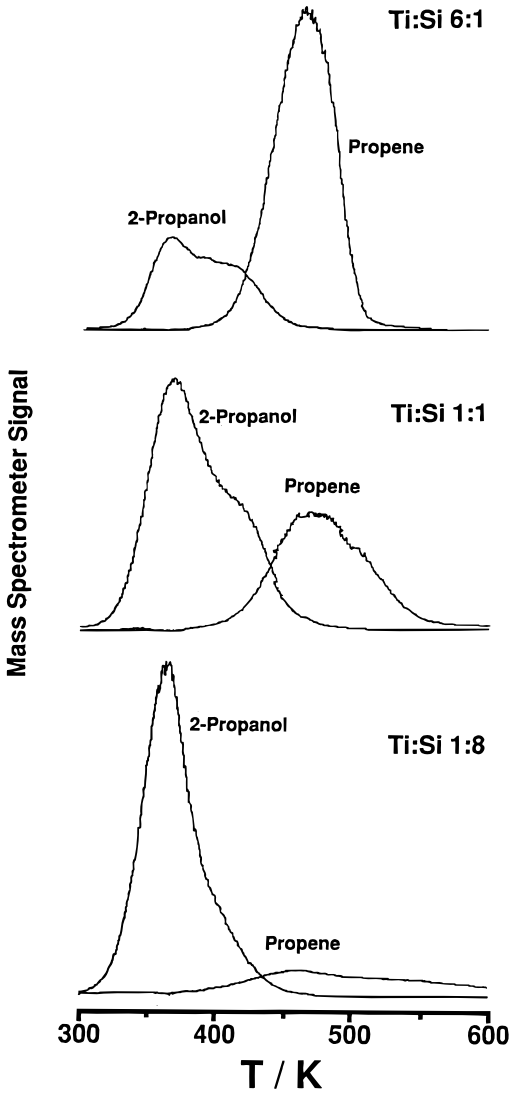

Figure 15. Results from the temperature-programmed reaction of 2-propanol on Ti−Si mixed oxides.[10]

neous mixed oxides that are the subject of this review. Biaglow et al. reported that the adsorption capacity of 2-propanol on titania (Degussa P25) was 4.0×10^{-6} mol m^{-2},[65] which compares favorably to 4.5×10^{-6} mol m^{-2} determined in our laboratory.[10] Kim et al. also found that 4.2×10^{-6} mol m^{-2} of 2-propanol adsorbed on low surface area (10 m^2 g^{-1}) anatase.[66] The adsorption capacity of titania prepared by hydrolysis of titanium isopropoxide is significantly higher than that of Degussa P25.[10] Kim et al. suggest that steric effects influence the adsorption capacity of 2-propanol on titania surfaces since methanol, ethanol, and *n*-propanol adsorb to a greater extent.[66] Evidently, the surfaces of high surface area synthetic titania must be highly irregular to allow for a greater adsorption capacity compared to P25.

Representative curves from the TPR of 2-propanol, illustrated in Figure 15, show that unreacted 2-propanol desorbed at relatively low temperatures, whereas propene desorbed at about 450−500 K. In addition, the fraction of 2-propanol that reacted to form propene was greatly affected by the composition of the mixed oxide. Silica-rich mixed oxides converted the lowest amounts of alcohol. Clearly, the adsorption capacities of the mixed oxides for 2-propanol are lower than that of pure titania and decrease with increasing Si content.

Summary of Results from Surface Characterization. The results from characterization of titania-silica mixed oxide surfaces must be interpreted in light of the bulk characterization studies discussed earlier. The number, type, and strength of surface acid sites on the mixed oxides are a strong function of the elemental composition. Explanations for the generation of surface acidity on mixed oxides have been proposed,[67,68] but perhaps the most frequently referred to hypothesis is that of Tanabe et al.[69] A major assumption of the hypothesis is that the coordination number of each metal cation in its pure oxide structure is retained when the metal oxides are chemically mixed. In addition, the coordination number of every oxygen in the mixed oxide is assumed to be the coordination number of oxygen in the pure component oxide that is present in the majority. According to the above assumptions, a charge difference must exist on the impurity cation when octahedrally coordinated titania is mixed with tetrahedrally coordinated silica. Tanabe et al. suggested that if the charge difference is positive, then the impurity cation will act as a Lewis acid site, whereas if the charge difference is negative, then surface protons will balance the excess negative charge, producing Bronsted acidity.[69] Thus, this hypothesis suggests that Lewis acidity will appear on titania-rich mixed oxides while Bronsted acidity will appear on silica-rich mixed oxides.

Two problems arise when this hypothesis is applied to Ti−Si mixed oxides. First, a positive charge on Si is calculated to appear for Ti-rich mixed oxides, but the hypothesis of Tanabe et al. does not require electroneutrality for this case.[69] As discussed above, Bronsted acid sites that are not normally present on pure titania appear on Ti-rich mixed oxides. We proposed that the positive charge difference that occurs when tetrahedral Si (in silica) mixes chemically with octahedral Ti (in titania) is balanced by hydroxyl groups, thus producing Bronsted acidity. It should be pointed out that other researchers have reported new Lewis sites on Ti-rich mixed oxides,[70] and they invoke the Tanabe hypothesis to explain the new acid sites. However, new Lewis sites may result from a greater fraction of exposed Ti atoms at the surface of their mixed oxides. Typically, the mixed oxides have much greater surface areas than pure titania. In addition, we calcined our materials at a relatively moderate temperature of 673 K. Higher calcination temperatures may expose additional Lewis acid sites.

A second problem that must be resolved is the dramatic decrease in surface acidity of the Si-rich mixed oxide samples. According to Tanabe et al.,[69] these materials should exhibit significant Bronsted acidity. Bulk characterization of Si-rich mixed oxides by EXAFS, XANES, UV, FT-IR, and Raman spectroscopies indicated that Ti atoms no longer reside in octahedral sites but instead substitute directly for Si atoms in tetrahedral sites.[9] Therefore, the charge difference calculated by Tanabe et al. for Si-rich mixed oxides is based on the incorrect assumption that Ti maintains its octahedral coordination environment. A charge balance on a Si-rich mixed oxide using the experimental finding that Ti isomorphously substitutes for Si reveals no charge difference at all. Therefore, little surface acidity is expected on the Si-rich materials, which is consistent

with the low reactivities of these materials in 2-propanol temperature-programmed reaction.

These results are also completely consistent with the lack of strong acidity in titanosilicalite molecular sieves. In these materials, Ti atoms substitute isomorphously for Si in the silicalite molecular sieve framework, thus creating unique sites for selective oxidation reactions with hydrogen peroxide. The lack of significant acidity on the titanosilicalites nearly eliminates unwanted acid-catalyzed side reactions during oxidation reactions.[71] Since all the titanium atoms in the molecular sieves are tetrahedrally coordinated, Bronsted acid sites are not expected on these materials. Indeed, infrared spectroscopy of pyridine adsorbed on titanium silicalite reveals only weak Lewis acid sites.[72]

As mentioned earlier, there is little agreement on the strengths and number densities of acid sites on mixed oxides. Surface acidity will be greatly affected by the synthesis procedure. Preparation methods involving coprecipitation of various reagents such as titanium tetrachloride and sodium silicate may leave residual ions on the catalyst surface after washing that might affect surface acidity.[60] In addition, rapid precipitation and high temperature calcination may result in the formation of separate titania and silica phases. However, strongly acidic Lewis sites may not be exposed on mixed oxide surfaces formed under relatively mild calcination temperatures. Treatment of materials at very high temperatures will dehydroxylate the surfaces more completely, thus exposing Lewis acid sites different from those present on the oxides after low temperature calcination. Since the acidity of mixed oxides depends strongly on atomic-level mixing and the degree of surface hydroxylation, the wide variety of results presented in the literature is not surprising. This observation has been reemphasized recently by Klein et al.[18]

V. Catalytic Reactions: Relationships between Structure and Activity

Titania-silica mixed oxides are often studied as catalysts for two broad classes of reactions: acid-catalyzed reactions and selective oxidation reactions. This section will describe the relationships between surface structure and catalytic activity for two representative reactions, alkene isomerization (an acid-catalyzed reaction) and alkene epoxidation (a selective oxidation reaction).

Isomerization of Butene. Titania-silica mixed oxides are known to catalyze the isomerization of 1-butene at higher specific rates than either silica or titania.[3−5] Titania-rich mixed oxides, in particular, were found to have the highest activities for the reaction.[3,4] Figure 16 shows the areal rate of butene isomerization as a function of catalyst composition. The Ti-rich catalyst was almost 4 times more active than pure titania and pure silica was essentially inactive. Since the cis/trans ratio of the product butenes is near unity over the mixed oxides, the reaction is assumed to be acid-catalyzed, proceeding through a 2-butyl carbonium ion intermediate. This conclusion is supported by the work of Ko et al., who found that treating a Ti−Si mixed oxide catalyst with water increased the specific activity of the sample for olefin isomerization.[4] Recent work by the same group has also found that Ti-rich mixed oxides are far more active for butene isomerization than pure titania or pure silica.[20,70] Nakabayashi concluded from IR spectroscopy of adsorbed pyridine that new Bronsted acid sites on a Ti−Si mixed oxide accounted for the increase in the butene isomeration rate compared to the pure metal oxides.[5] Since Bronsted acidity was detected on all the mixed oxides, titania-rich and silica-rich, and since the Ti-rich mixed oxides were the most active for butene isomerization, we concluded that 1-butene isomerization is enhanced by the formation of new Bronsted acid sites not present on pure titania. However, the weak Bronsted acid sites on the silica-rich mixed oxides are apparently not effective for butene isomerization.

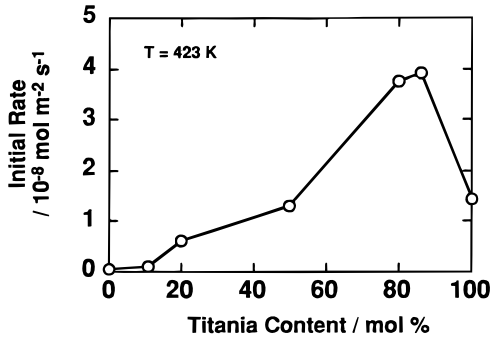

Figure 16. Influence of catalyst composition on the specific rate of 1-butene isomerization.[10]

Even though some issues regarding acid site density and strength are still unresolved, an unambiguous relationship between acidity and catalytic activity exists for butene isomerization. The differences in isomerization rates reported by separate laboratories can easily be explained by the variability in materials preparation. As discussed in the previous section, acid sites on these mixed oxides result from local charge imbalances that arise when chemically dissimilar oxides are mixed. Thus, the degree of atomic-level mixing is absolutely critical to the overall catalytic performance of the resulting mixed oxide.

Epoxidation of Hexene. The effectiveness of Ti−Si mixed oxides for selective oxidation reactions with organic hydroperoxides has been known for many years.[8] Typically, a low weight percent of titanium is supported on silica to form the active material. Pure silica is considered inert in these reactions whereas pure titania often decomposes the peroxide unselectively. However, in some cases, titania can show minimal activity for selective oxidation products. For example, Hutter et al. reported that pure titania catalyzed epoxidation of cyclohexene by cumene hydroperoxide.[73]

The variation of epoxidation activity with Ti−Si mixed oxide composition reveals important characteristics of this selective oxidation reaction. Reactivity results for the epoxidation of 1-hexene with *tert*-butylhydroperoxide (TBHP) on Ti−Si mixed oxide catalysts are summarized in Table 4.[11] The TBHP efficiency is defined as the percentage of 1,2-epoxyhexane produced compared to TBHP consumed. The activity and selectivity of Ti−Si mixed oxide catalysts were higher than pure titania, but depended strongly on the composition. The silica-rich mixed oxide was the most effective catalyst for epoxidation.

The characterization results of the Ti−Si mixed oxides indicated that most of the Ti atoms in Si-rich mixed oxides reside in tetrahedral sites formed by direct

Table 4. Comparison of 1-Hexene Epoxidation Activity over Ti−Si Mixed Oxides [11a]

sample	TBHP conversion/%	TBHP efficiency/%
blank	2.2	0
TiO_2	15.5	10.8
Ti:Si 6:1	34.7	20.8
Ti:Si 1:1	23.5	27.5
Ti:Si 1:8	37.6	77.2
meso-TiSi−20	64.1	89.6
meso-TiSi−40	86.4	84.1

[a] Conditions: 48 mmol of 1-hexene, 4.8 mmol of TBHP, 50 mg of catalyst, 353 K, 4 h.

substitution into silica.[9] The Ti sites for selective oxidation in TS-1 catalysts are known to be tetrahedrally coordinated Ti atoms located in framework sites normally occupied by Si.[32] Similarly, the highly effective catalytic sites for selective epoxidation on the Ti−Si mixed oxides are likely due to tetrahedral Ti atoms in a silica lattice, which is in agreement with the study of Imamura et al.[74] Hutter et al. proposed that two types of sites exist on Ti−Si mixed oxides: one type associated with titania microdomains, and a second type associated with isolated Ti, which is the highly active site.[73] Recently, pure titanium oxides were studied as catalysts for epoxidation of octene with TBHP.[75] Ultrafine titania formed by hydrolysis of titanium isopropoxide, without high-temperature calcination, showed activity for epoxidation at 363 K. High-temperature calcination of these catalysts eliminated the selective oxidation sites. The authors proposed that unsaturated Ti sites are necessary for selective oxidation and that silica supports are ideal for maintaining the highly active tetrahedral Ti site.

If the isolated Ti atoms in the tetrahedral silica matrix are the most active sites in these materials, then very low concentrations of Ti in extremely high surface area silicas should be the best catalysts. The last two entries of Table 4 show the catalytic activity of Ti atoms incorporated into mesoporous silica prepared by a direct synthesis method involving liquid-crystal templating. Characterization results indicated that the Ti atoms are isolated in the silica matrix.[11] As expected, these materials were the most active and selective of the mixed oxides reported in Table 4. The direct synthesis method used to prepare these samples does not guarantee that all of the Ti atoms are exposed to the surface. Any titanium that is buried in the bulk matrix is inactive for selective oxidation reactions. Recently, a new postsynthetic treatment of high surface area silica has been developed to graft isolated Ti atoms onto the silica surface.[29] When compared on a per Ti atom basis, these new materials are the most active, amorphous solid epoxidation catalysts yet reported.

Titanium-substituted silicalite, TS-1, is an extremely effective catalyst for selective epoxidation of small alkenes with aqueous hydrogen peroxide. A unique capability of this catalyst is that high activitiy and selectivity for selective oxidation can be sustained in the presence of water and polar solvents. Soluble epoxidation catalysts are strongly inhibited by water, presumably due to strong coordination with the active site.

Klein et al. evaluated the surface polarities of microporous titania-silica mixed oxides and TS-1, based on the competitive adsorption of water and octane.[18] For samples of about the same Ti loading (∼2%), the amorphous mixed oxide had a 10:1 preference of water over octane, whereas TS-1 had a 3:1 preference of octane over water. The significant hydrophobicity of TS-1 may account for its excellent catalytic activity in aqueous solutions.

Table 5. Effect of Cosolvent on 1-Hexene Epoxidation[11a]

cosolvent	TBHP conversion/%	TBHP efficiency/%
water	14.9	1.87
methanol	29.9	7.5
acetone	38.7	18.7
n-butanol	17.9	68.8
methy ethyl ketone	37.1	37.6
decane	37.6	77.2
isopropyl ether	27.2	79.5
1,1,2,2-tetrachoroethane	40.1	76.7
2,4,6-tri-*tert*-butylphenol[b]	48.5	80.8

[a] Conditions: 48 mmol of 1-hexene, 4.8 mmol of TBHP, 50 mg of Ti:Si 1:8 catalyst, volume ratio of decane to cosolvent = 2, 353 K, 4 h. [b] Free radical inhibitor, 0.48 mmol added.

The influence of cosolvents on 1-hexene reaction with TBHP catalyzed by a Si-rich mixed oxide is shown in Table 5. The reaction was greatly retarded by water, which is similar to the behavior of soluble metal catalysts[76] and is anticipated from the surface polarity measurements of Klein et al.[18] Inhibition by water can be attributed to its strong coordination with the surface of the mixed oxide, which blocks the active sites from reactant molecules. The presence of small alcohol and ketone compounds also decreased the selectivity of TBHP to epoxide product, but not to the same extent as added water. However, as less polar solvent molecules were added, the negative effect on epoxidation diminished. Addition of a free radical inhibitor, 2,4,6-tri-*tert*-butylphenol, to the reaction solution did not reduce the conversion or efficiency, implying that the epoxidation does not proceed through a radical mechanism in the liquid phase. Recent studies on low-weight-percent Ti in mesoporous silica showed that the measured rates of epoxidation with aqueous hydrogen peroxide are far lower than those typically reported for TS-1.[11] Even though multiple characterization studies indicate the similarity of the tetrahedral Ti site in amorphous mixed oxides and TS-1, the larger irregular pores of the amorphous materials that contain silanol groups appear to inadequately exclude water or other highly polar molecules.

VI. Conclusions

Variations in synthesis procedure can profoundly affect the homogeneity of component mixing at the atomic level. Since Ti and Si alkoxide precursors do not hydrolyze and condense at the same rate, small titania-rich domains may form in the mixed oxides. The inequivalence of hydrolysis rates can be partially mitigated by prehydrolysis of the slower reacting component or by complexing the faster reacting component. Nevertheless, characterization results of alkoxide-derived mixed oxides are fairly consistent, regardless of preparation procedure. Titanium-rich mixed oxides tend to have silica located preferentially at the surface. The charge imbalance resulting from atomic level mixing of 4-coordinated Si^{4+} and 6- (or 5-) coordinated Ti^{4+} forms new, catalytically active, acid sites that are not present on either of the pure oxide surfaces. Silica-rich mixed

oxides are much less acidic due to the substitution of many titanium atoms into the tetrahedral sites normally occupied by silicon, thus eliminating the charge imbalance responsible for the acidity of Ti-rich mixed oxides. The isolation of tetrahedrally coordinated Ti atoms in silica correlates with the activity and selectivity of alkene epoxidation reactions, which suggests that those atoms are the active sites for oxidation. Clearly, the method of synthesis, which affects the degree of homogeneity of component mixing, plays a crucial role in determining the surface character of the final catalytic materials.

Acknowledgments are made to the National Science Foundation for a Young Investigator Award (CTS-9257306) and to the donors of the Petroleum Research Fund, administered by the American Chemical Society (ACS-PRF 28260-AC5).

References

(1) Schultz, P. C.; Smyth, H. T. In *Amorphous Materials*; Douglas, E. W., Ellis, B., Eds.; Wiley: London, 1972; p 453.
(2) Evans, D. L. *J. Non-Cryst. Solids* **1982**, *52*, 115.
(3) Itoh, M.; Hattori, H.; Tanabe, K. *J. Catal.* **1974**, *35*, 225.
(4) Ko, E. I.; Chen, J. P.; Weissman, J. G. *J. Catal.* **1987**, *105*, 511.
(5) Nakabayashi, H. *Bull. Chem. Soc. Jpn.* **1992**, *65*, 914.
(6) Sohn, J. R.; Jang, H. J. *J. Catal.* **1991**, *132*, 563.
(7) Imamura, S.; Tarumoto, H.; Ishida, S. *Ind. Eng. Chem. Res.* **1989**, *28*, 1449.
(8) Wulff, H P. U.S. Patent 3,923,843, 1975. Wulff, H. P.; Wattimena, F. U.S. Patent 4,367,342, 1983.
(9) Liu, Z.; Davis, R. J. *J. Phys. Chem.* **1994,** *98*, 1253.
(10) Liu, Z.; Tabora, J.; Davis, R. J. *J. Catal.* **1994,** *149*, 117.
(11) Liu, Z.; Crumbaugh, G. M.; Davis, R. J. *J. Catal.* **1996,** *159*, 83.
(12) Taramasso, M.; Perego, G.; Notari, B. US Patent 4,410,501, 1983.
(13) Notari, B. *Adv. Catal.* **1996**, *41*, 253.
(14) Greegor, R. B.; Lytle, F. W.; Sandstrom, D. R.; Wong, J.; Schultz, P. *J. Non-Cryst. Solids* **1983**, *55*, 27.
(15) Schraml-Marth, M.; Walther, K. L.; Wokaun, A.; Handy, B. E.; Baiker, A. *J. Non-Cryst. Solids* **1992**, *143*, 93.
(16) Walther, K. L.; Wokaun, A.; Handy, B. E.; Baiker, A. *J. Non-Cryst. Solids* **1991**, *134*, 47.
(17) Ko, E. I. *Chemtech* **1993**, *April*, 31.
(18) Klein, S.; Thorimbert, S.; Maier, W. F. *J. Catal.* **1996**, *163*, 476.
(19) Best, M. F.; Condrate, R. A. *J. Mater. Sci. Lett.* **1985**, *4*, 994.
(20) Miller, J. B.; Johnston, S. T.; Ko, E. I. *J. Catal.* **1994**, *150*, 311.
(21) Dutoit, D. C. M.; Schneider, M.; Baiker, A. *J. Catal.* **1995**, *153*, 165.
(22) Miller, J. B.; Mathers, L. J.; Ko, E. I. *J. Mater. Chem.* **1995**, *5*, 1759.
(23) Beck, J. S.; Vartuli, J. C.; Roth, W. J.; Leonowicz, M. E.; Kresge, C. T.; Schmitt, K. D.; Chu, C. T.-W.; Olson, D. H.; Sheppard, E. W.; McCullen, S. B.; Higgins, J. B.; Schlenker, J. L. *J. Am. Chem. Soc.* **1992**, *114*, 10834.
(24) Corma, A.; Navarro, M. T.; Pariente, J. P. *J. Chem. Soc., Chem. Commun.* **1994**, 147.
(25) Tanev, P. T.; Chibwe, M.; Pinnavaia, T. J. *Nature* **1994**, *368*, 321.
(26) Zhang, W.; Froba, M.; Wang, J.; Tanev, P. T.; Wong, J.; Pinnavaia, T. J. *J. Am. Chem. Soc.* **1996**, *118*, 9164.
(27) Gontier, S.; Tuel, A. *Zeolites* **1995**, *15*, 601.
(28) Branton, P. J.; Hall, P. G.; Sing, K. S. W. *J. Chem. Soc., Chem. Commun.* **1993**, 1257.
(29) Maschmeyer, T.; Rey, F.; Sankar, G.; Thomas, J. M. *Nature* **1995**, *378*, 159.
(30) Waychunas, G. A. *Am. Mineral.* **1987**, *72*, 89.
(31) Davis, R. J.; Liu, Z.; Tabora, J. E.; Wieland, W. S. *Catal. Lett.* **1995**, *34*, 101.
(32) Pei, S.; Zajac, G. W.; Kaduck, J. A.; Faber, J.; Boyanov, B. I.; Duck, D.; Fazzini, D.; Morrison, T. I.; Yang, D. S. *Catal. Lett.* **1993**, *21*, 333.
(33) Sandstrom, D. R.; Lytle, F. W.; Wei, P. S. P; Greegor, R. B.; Wong, J.; Schultz, P. *J. Non-Cryst. Solids* **1980**, *41*, 201.
(34) Emili, M.; Incoccia, L.; Mobilio, S.; Fagherazzi, G.; Guglielmi, M. *J. Non-Cryst. Solids* **1985**, *74*, 129.
(35) Neurock, M.; Manzer, L. E., *Chem. Commun.* **1996**, 1133.
(36) Schultz, E.; Ferrini, C.; Prins, R. *Catal. Lett.* **1992**, *14*, 221.
(37) Anpo, M.; Nakaya, H.; Kodama, S.; Kubokawa, Y.; Domen, K.; Onishi, T. *J. Phys. Chem.* **1986**, *90*, 1633.
(38) Henglein, A. *Chem. Rev. (Washington, D.C.)* **1989**, *89*, 1861.
(39) Davis, R. J. *Chem. Mater.* **1992**, *4*, 1410.
(40) Reddy, J. S.; Kumar, R. *J. Catal.* **1991**, *130*, 440.
(41) Wang, Y.; Suna, A.; Mahler, W.; Kasowski, R. *J. Chem. Phys.* **1987**, *87*, 7315.
(42) Yoneyama, H.; Haga, S.; Yamanaka, S. *J. Phys. Chem.* **1989,** *93*, 4833.
(43) Kasinski, J. J.; Gomez-Jahn, L. A.; Faran, K. J.; Gracewski, S. M.; Dwayne Miller, R. J. *J. Chem. Phys.* **1989**, *90*, 1253.
(44) Parker, J. C.; Siegel, R. W. *J. Mater. Res.* **1990**, *5*, 1246.
(45) Parker, J. C.; Siegel, R. W. *Appl. Phys. Lett.* **1990**, *57*, 943.
(46) Arashi, H. *J. Phys. Chem. Solids*. **1992**, *53*, 355.
(47) Melendres, C. A.; Narayanasamy, A.; Maroni, V. A.; Siegel, R. W. *J. Mater. Res*. **1989**, *4*, 1246.
(48) Neumann, R.; Levin-Elad, M. *J. Catal.* **1997**, *166*, 206.
(49) Lippmaa, E.; Magi, M.; Samoson, A.; Engelhardt, G.; Grimmer, A. R. *J. Am. Chem. Soc.* **1980**, *102*, 4889.
(50) Sindorf, D. W.; Maciel, G. E. *J. Am. Chem. Soc.* **1983**, *105*, 1487.
(51) Wies, C.; Meise-Gresch, K.; Muller-Warmuth; Beier, W.; Goktas, A. A.; Frischat, H. G. *Phys. Chem. Glasses* **1990**, *31*, 138.
(52) Stakheev, A. Yu.; Shpiro, E. S.; Apijok, J. *J. Phys. Chem.* **1993**, *97*, 5668.
(53) Liu, Z. Ph.D. Dissertation, University of Virginia, 1995.
(54) Lassaletta, G.; Fernandez, A.; Espinos, J. P.; Gonzalez-Elipe, A. R. *J. Phys. Chem.* **1995**, *99*, 1484.
(55) Odenbrand, C. U. I.; Andersson, S. L. T.; Andersson, L. A. H.; Brandin, J. G. M.; Busca, G. *J. Catal.* **1990**, *125*, 541.
(56) Primet, M.; Pichat, P.; Mathieu, M.-V. *J. Phys. Chem.* **1971**, *75*, 1216.
(57) Busca, G.; Saussey, H.; Saur, O.; Lavalley, J. C.; Lorenzelli, V. *Appl. Catal.* **1985**, *14*, 245.
(58) Primet, M.; Pichat, P.; Mathieu, M.-V. *J. Phys. Chem.* **1971**, *75*, 1221.
(59) Dines, T. J.; Rochester, C. H.; Ward, A. M. *J. Chem. Soc., Faraday Trans.* **1991**, *87*, 643.
(60) Odenbrand, C. U. I.; Brandin, J. G. M.; Busca, G. *J. Catal.* **1992**, *135*, 505.
(61) Shibata, K.; Kiyoura, T.; Kitagawa, J.; Sumiyoshi, T.; Tanabe, K. *Bull. Chem. Soc. Jpn.* **1973**, *46*, 2985.
(62) Nakabayashi, H.; Kakuta, N.; Ueno, A. *Bull. Chem. Soc. Jpn.* **1991**, *64*, 2428.
(63) Sabu, K. R. P.; Rao, K. V. C.; Nair, C. G. R. *Bull. Chem. Soc. Jpn.* **1991**, *64*, 1920.
(64) Juskelis, M. V.; Slanga, J. P.; Roberie, T. G.; Peters, A. W. *J. Catal.* **1992**, *138*, 391.
(65) Biaglow, A. I.; Gorte, R. J.; Srinivasan, S.; Datye, A. K. *Catal. Lett.* **1992**, *13*, 313.
(66) Kim, K. S.; Barteau, M. A.; Farneth, W. E. *Langmuir* **1988**, *4*, 533.
(67) Kung, H. H. *J. Solid State Chem.* **1984**, *52*, 191.
(68) Kataoka, T.; Dumesic, J. A. *J. Catal.* **1988**, *112*, 66.
(69) Tanabe, K.; Sumiyoshi, T.; Shibata, K.; Kiyoura, T.; Kitagawa, J. *Bull. Chem. Soc. Jpn.* **1974**, *47*, 1064.
(70) Miller, J. B.; Ko, E. I. *J. Catal.* **1996**, *159*, 58.
(71) Clerici, M. G.; Bellussi, G.; Romano, U. *J. Catal.* **1991**, *129*, 159.
(72) Bittar, A.; Adnot, A.; Sayari, A.; Kaliaguine, S. *Res. Chem. Intermed.* **1992**, *18*, 49.
(73) Hutter, R.; Mallat, T.; Baiker, A. *J. Catal.* **1995**, *153*, 177.
(74) Imamura, S.; Nakai, T.; Kanai, H.; Ito, T. *J. Chem. Soc., Faraday Trans.* **1995**, *91*, 1261.
(75) Imamura, S.; Nakai, T.; Utani, K.; Kanai, H. *J. Catal.* **1996**, *161*, 495.
(76) Sheldon, R. A. *J. Mol. Catal.* **1980**, *7*, 107.

CM970314U